



## Weakened growth of cropland N<sub>2</sub>O emissions in China associated with nationwide policy interventions

Journal:	<i>Global Change Biology</i>
Manuscript ID	Draft
Wiley - Manuscript type:	Primary Research Articles
Date Submitted by the Author:	n/a
Complete List of Authors:	<p>Shang, Ziyin; Peking University, Sino-France Institute of Earth Systems Science, Laboratory for Earth Surface Processes, College of Urban and Environmental Sciences; University of Aberdeen, Institute of Biological and Environmental Science</p> <p>Zhou, Feng; Peking University, Ecology</p> <p>Smith, Pete; University of Aberdeen, Institute of Biological and Environmental Science</p> <p>Saikawa, Eri ; Emory University, Department of Environmental Sciences</p> <p>Ciais, Philippe; Laboratory for Climate Sciences and the Environment (LSCE)</p> <p>CHANG, Jinfeng; Laboratory for Climate Sciences and the Environment (LSCE)</p> <p>Tian, Hanqin; Auburn University, School of Forestry and Wildlife Sciences</p> <p>Del Grosso, Stephen J; USDA ARS, Soil Management and Sugar Beet Research</p> <p>Ito, Akihiko; National Institute for Environmental Studies, Center for Global Environmental Research</p> <p>Chen, Minpeng; Renmin University of China, School of Agricultural Economics and Rural Development</p> <p>Wang, Qihui; Peking University, Sino-France Institute of Earth Systems Science, Laboratory for Earth Surface Processes, College of Urban and Environmental Sciences</p> <p>BO, YAN; Peking University</p> <p>Cui, Xiaoqing; Peking University, Sino-France Institute of Earth Systems Science, Laboratory for Earth Surface Processes, College of Urban and Environmental Sciences</p> <p>Castaldi, Simona; Universita degli Studi della Campania Luigi Vanvitelli, Dipartimento di Scienze e Tecnologie Ambientali Biologiche e Farmaceutiche</p> <p>Juszczak, Radoslaw; Poznan University of Life Sciences, Department of Meteorology</p> <p>Kasimir, Åsa; University of Gothenburg, Department of Earth Sciences</p> <p>Magliulo, Vincenzo; National Research Council of Italy, Institute for Mediterranean Agriculture and Forest Systems</p> <p>Medinets, Sergiy; Odessa National I. I. Mechnikov University, Regional Centre for Integrated Environmental Monitoring and Ecological Studies</p> <p>Medinets, Volodymyr; Odessa National I.I. Mechnikov University, Regional Centre for Integrated Environmental Monitoring and Ecological Studies</p> <p>Rees, Bob; Scotland's Rural College</p>

	Wohlfahrt, Georg; University of Innsbruck, Institute of Ecology Sabbatini, Simone; University of Tuscia, DIBAF
Keywords:	Nitrous oxide, agricultural soils, emission inventory, flux upscaling, agricultural management, process-based model, temporal trend, spatial pattern
Abstract:	<p>China has experienced rapid agricultural development over recent decades, accompanied by increased fertilizer consumption in croplands, yet the trend and drivers of the associated nitrous oxide (N<sub>2</sub>O) emissions remain uncertain. The primary sources of this uncertainty are the coarse spatial variation of activity data and the incomplete model representation of N<sub>2</sub>O emissions in response to agricultural management. Here we provide new data-driven estimates of cropland N<sub>2</sub>O emissions across China in 1990-2014, compiled using a global cropland-N<sub>2</sub>O flux observation dataset, nationwide survey-based reconstruction of N-fertilization and irrigation, and an updated nonlinear model. In addition, we have evaluated the drivers behind changing cropland N<sub>2</sub>O patterns using an index decomposition analysis approach. We find that China's annual cropland-N<sub>2</sub>O emissions increased on average by 11.2 Gg N yr<sup>-2</sup> (<math>P &lt; 0.001</math>) from 1990 to 2003, after which emissions plateaued until 2014 (2.8 Gg N yr<sup>-2</sup>, <math>P = 0.02</math>), consistent with the output from an ensemble of process-based terrestrial biosphere models (TBMs). The slowdown of the increase in cropland-N<sub>2</sub>O emissions after 2003 was pervasive across two thirds of China's sowing areas. This change was mainly driven by the nationwide reduction of N-fertilizer applied per area, partially due to the prevalence of the Nationwide Soil Testing and Formulation Fertilization Program that was launched in the early 2000s. This reduction has almost offset the N<sub>2</sub>O emissions induced by policy-driven expansion of sowing areas, particularly in the Northeast Plain and the lower Yangtze River Basin. Our results underline the importance of high-resolution activity data and adoption of nonlinear model of N<sub>2</sub>O emission for capturing cropland-N<sub>2</sub>O emission changes. Improving the representation of policy interventions is also recommended for future projections.</p>

1 **Weakened growth of cropland N<sub>2</sub>O emissions in China associated**  
2 **with nationwide policy interventions**

3 Ziyin Shang<sup>1, 2</sup>, Feng Zhou<sup>1\*</sup>, Pete Smith<sup>2</sup>, Eri Saikawa<sup>3</sup>, Philippe Ciais<sup>4</sup>, Jinfeng Chang<sup>4</sup>, Hanqin Tian<sup>5</sup>,  
4 Stephen J. Del Grosso<sup>6</sup>, Akihiko Ito<sup>7</sup>, Minpeng Chen<sup>8</sup>, Qihui Wang<sup>1</sup>, Yan Bo<sup>1</sup>, Xiaoqing Cui<sup>1</sup>, Simona  
5 Castaldi<sup>9</sup>, Radoslaw Juszczak<sup>10</sup>, Åsa Kasimir<sup>11</sup>, Enzo Magliulo<sup>12</sup>, Sergiy Medinets<sup>13</sup>, Volodymyr Medinets<sup>13</sup>,  
6 Robert M. Rees<sup>14</sup>, Georg Wohlfahrt<sup>15</sup>, Simone Sabbatini<sup>16</sup>

7

8 <sup>1</sup>Sino-France Institute of Earth Systems Science, Laboratory for Earth Surface Processes, College of Urban  
9 and Environmental Sciences, Peking University, Beijing, 100871, P.R. China.

10 <sup>2</sup>Institute of Biological and Environmental Sciences, University of Aberdeen, 23 St Machar Drive, Aberdeen  
11 AB24 3UU, UK.

12 <sup>3</sup>Department of Environmental Sciences, Emory University, Atlanta, Georgia 30322, USA.

13 <sup>4</sup>Laboratoire des Sciences du Climat et de l'Environnement, CEA CNRS UVSQ, 91191 Gif-sur-Yvette,  
14 France

15 <sup>5</sup>International Center for Climate and Global Change Research, School of Forestry and Wildlife Sciences,  
16 Auburn University, Auburn, Alabama, USA

17 <sup>6</sup>Soil Management and Sugar Beet Research, USDA Agricultural Research Service, 2150 Centre Ave., Fort  
18 Collins, CO 80526, USA

19 <sup>7</sup>Center for Global Environmental Research, National Institute for Environmental Studies, Tsukuba, Japan

20 <sup>8</sup>School of Agricultural Economics and Rural Development, Renmin University of China, Beijing, 100872,  
21 P.R. China.

22 <sup>9</sup>Dipartimento di Scienze e Tecnologie Ambientali Biologiche e Farmaceutiche, Università degli Studi della  
23 Campania "Luigi Vanvitelli", via Vivaldi 43, 81100 Caserta, Italy.

24 <sup>10</sup>Department of Meteorology, Poznan University of Life Sciences, 60-649 Poznan, Poland.

25 <sup>11</sup>Department of Earth Sciences, University of Gothenburg, Gothenburg, Sweden.

26 <sup>12</sup>13I SAFOM-CNR, Institute for Mediterranean Agricultural and Forest Systems, National Research  
27 Council, Via Patacca 85, 80056 Ercolano (NA), Italy

28 <sup>13</sup>Regional Centre for Integrated Environmental Monitoring and Ecological Researches, Odessa National I.  
29 I. Mechnikov University (ONU), Mayakovskogo Lane 7, 65082 Odessa, Ukraine.

30 <sup>14</sup>Scotland's Rural College (SRUC), Edinburgh EH9 3JG, Scotland, UK.

31 <sup>15</sup>Institute of Ecology, University of Innsbruck, Sternwartestrasse 15, Innsbruck, Austria.

32 <sup>16</sup>Department for Innovation in Biological, Agro-food and Forest Systems (DIBAF), University of Tuscia,  
33 via S. Camillo de Lellis s.n.c., 01100 Viterbo, Italy.

34

35 **\*Corresponding Author**

36 Phone: +86 10 62756511, Fax: +86 10 62756560; Email: [zhouf@pku.edu.cn](mailto:zhouf@pku.edu.cn).

## 37 **ABSTRACT**

38 China has experienced rapid agricultural development over recent decades, accompanied by  
39 increased fertilizer consumption in croplands, yet the trend and drivers of the associated nitrous  
40 oxide (N<sub>2</sub>O) emissions remain uncertain. The primary sources of this uncertainty are the coarse  
41 spatial variation of activity data and the incomplete model representation of N<sub>2</sub>O emissions in  
42 response to agricultural management. Here we provide new data-driven estimates of cropland  
43 N<sub>2</sub>O emissions across China in 1990-2014, compiled using a global cropland-N<sub>2</sub>O flux  
44 observation dataset, nationwide survey-based reconstruction of N-fertilization and irrigation,  
45 and an updated nonlinear model. In addition, we have evaluated the drivers behind changing  
46 cropland N<sub>2</sub>O patterns using an index decomposition analysis approach. We find that China's  
47 annual cropland-N<sub>2</sub>O emissions increased on average by 11.2 Gg N yr<sup>-2</sup> ( $P < 0.001$ ) from 1990  
48 to 2003, after which emissions plateaued until 2014 (2.8 Gg N yr<sup>-2</sup>,  $P = 0.02$ ), consistent with  
49 the output from an ensemble of process-based terrestrial biosphere models (TBMs). The  
50 slowdown of the increase in cropland-N<sub>2</sub>O emissions after 2003 was pervasive across two  
51 thirds of China's sowing areas. This change was mainly driven by the nationwide reduction of  
52 N-fertilizer applied per area, partially due to the prevalence of the Nationwide Soil Testing and  
53 Formulation Fertilization Program that was launched in the early 2000s. This reduction has  
54 almost offset the N<sub>2</sub>O emissions induced by policy-driven expansion of sowing areas,  
55 particularly in the Northeast Plain and the lower Yangtze River Basin. Our results underline  
56 the importance of high-resolution activity data and adoption of nonlinear model of N<sub>2</sub>O  
57 emission for capturing cropland-N<sub>2</sub>O emission changes. Improving the representation of policy  
58 interventions is also recommended for future projections.

59 **Keywords:** Nitrous oxide; agricultural soils; emission inventory; flux upscaling; agricultural  
60 management; process-based model; temporal trend; spatial pattern

For Review Only

## 61 **1. Introduction**

62 Nitrous oxide (N<sub>2</sub>O) is a potent greenhouse gas, with a global warming potential 265~298 times  
63 greater than that of CO<sub>2</sub> over a 100-year time horizon (Myhre et al., 2013). Its emissions are  
64 recognized as the most important ozone-depleting substance (Ravishankara, Daniel, &  
65 Portmann, 2009). Accumulating evidence points to croplands as the largest global source  
66 (>40%) of anthropogenic N<sub>2</sub>O (Paustian et al., 2016). Global cropland N<sub>2</sub>O emissions are  
67 projected to increase by ~50% from 2010 to 2050, due to the future intensification and  
68 expansion of cropland production (Alexandratos & Bruinsma, 2012). Reducing cropland N<sub>2</sub>O  
69 emissions is a key mitigation option for limiting climate warming, especially in relation to  
70 recently developed policy objectives relating to climate change and concerns regarding ozone  
71 depletion (Allen et al. 2018). However, high spatial and temporal variability makes the  
72 estimation of cropland N<sub>2</sub>O emissions notoriously difficult (e.g., quantity, pattern, trend)  
73 (Paustian et al., 2016), resulting in large discrepancies between bottom-up and top-down  
74 approaches (Tian et al., 2016).

75

76 One of the sources of uncertainty is the model structure of bottom-up approaches that consider  
77 a linear response of N<sub>2</sub>O emissions to N application rate, as recommended in the Tier 1 method  
78 for a national N<sub>2</sub>O inventory by the Intergovernmental Panel on Climate Change (IPCC, 2006).  
79 Recent synthesis of field observations suggests that N<sub>2</sub>O emissions respond nonlinearly to an  
80 increasing N application rate (Philibert, Loyce, & Makowski, 2012; Shcherbak, Millar, &  
81 Robertson, 2014; Song et al. 2018) This nonlinear response was partially ascribed to the fact  
82 that high ammonium ion concentrations from urea hydrolysis inhibits nitrite transformation to  
83 nitrate (Ma, Shan, & Yan, 2015), resulting in nitrite accumulation which is subsequently  
84 emitted as N<sub>2</sub>O. Philibert et al. (2012) proposed a nonlinear model with fixed parameters, which  
85 improved the predictive performance of N<sub>2</sub>O flux. This model was further improved by using

86 random parameters from a more recent and a larger field observation dataset of N<sub>2</sub>O flux  
87 (Gerber et al., 2016). In addition to the nonlinear response of emissions to N inputs,  
88 microbially-mediated N<sub>2</sub>O is also strongly dependent on climate and soil properties (Perlman,  
89 Hijmans, & Horwath, 2014). A spatially-referenced nonlinear model was therefore developed  
90 to simulate N<sub>2</sub>O emissions in response to fertilizer N application rate ( $N_{\text{rate}}$ ) under various  
91 environmental or management-related conditions (Zhou et al., 2015). Comparison between  
92 models showed that such models outperformed nonlinear models with fixed or random  
93 parameters (Zhou et al., 2015).

94

95 The accuracy of simulating N<sub>2</sub>O emissions is dependent on the representation of model  
96 parameters and the spatial aggregation of agricultural activity data. For example, a spatially-  
97 referenced nonlinear model (Zhou et al., 2015) calibrated against observations in China was  
98 able to better capture the variations of N<sub>2</sub>O emissions on sites with similar conditions to the  
99 calibration dataset, but was unable to reproduce emissions at other sites. To improve the  
100 performance of diagnostic models at a regional scale, field observations representative of a  
101 wide range of environmental and management-related variables are required. In addition, N<sub>2</sub>O  
102 emission models are sensitive to the degree of spatial aggregation in fertilizer and irrigation  
103 data. Uncertainty of input data is expected to increase with decreasing spatial scale without  
104 altering spatial differences in fertilizer and irrigation applications (Gerber et al., 2016).  
105 Although the spatial resolution of management-related data is improving, mainly by evenly  
106 disaggregating national-scale data into gridded maps (Lu & Tian, 2017; Zhang et al., 2017),  
107 long-term, high-resolution maps of cropland-specific N-fertilizers and irrigation inputs are not  
108 yet available at the global or regional scale.

109

110 China is currently the largest emitters of anthropogenic N<sub>2</sub>O emissions globally (Zhou et al.,

111 2014). Over the past decades, this source in China increased with N-fertilizer use, accounting  
112 for over 20% of global cropland-N<sub>2</sub>O emissions from IPCC Tier 1 inventories (FAO, 2018;  
113 Janssens-Maenhout et al., 2019; Winiwarter, Höglund-Isaksson, Klimont, Schöpp, & Amann,  
114 2018). China is a large country with contrasting crop production systems, climate and soil types,  
115 where the patterns of N<sub>2</sub>O emissions are poorly understood compared to some developed  
116 countries (Zou et al., 2010; Zhou et al., 2015; Yue et al., 2018). In the last decade, process-  
117 based models (e.g., DNDC, DAYCENT, DLEM), used to produce Tier 3 IPCC estimates,  
118 simulated global and regional cropland-N<sub>2</sub>O emissions using sub-national N inputs from China  
119 (Li et al, 2001; Tian et al., 2019; Yue et al., 2019). These models are arguably more realistic  
120 than the Tier 1 approach because they account for climatic and soil variabilities. Although  
121 multi-model ensemble may reduce some errors across individual models through a broader  
122 integration of model processes (Tian et al., 2019), these individual models have rarely been  
123 validated by observations across contrasting environmental and management-related  
124 conditions (Ehrhardt et al., 2017), leading to large uncertainties not only in estimating emission  
125 trends, but also in identifying underlying drivers.

126

127 To address these knowledge gaps, we re-estimate the spatial pattern and temporal trend of  
128 cropland N<sub>2</sub>O emissions across China in 1990-2014. We advance the estimation of spatially-  
129 explicit, long-term cropland N<sub>2</sub>O emissions in China by using an updated version of the  
130 spatially-referenced nonlinear model (Zhou et al., 2015) with high-resolution, crop-specific  
131 gridded datasets of N-fertilizer and irrigation uses. First, the model was updated through re-  
132 calibration with N<sub>2</sub>O emission observations three times more than previous dataset. Second,  
133 maps (1-km) of crop-specific N-fertilization and irrigation application rates across Chin were  
134 collated, based on a compilation of sub-national statistics or surveys (Zhou et al., 2014; Zou et  
135 al. 2018), which differ from previous datasets based on downscaling of national totals (Lu &



136 Tian, 2017; Janssens-Maenhout et al., 2017) or modeling (Flörke, Schneider, & McDonald,  
137 2018). Finally, using one type of index decomposition analysis (Ang, 2015), we separated the  
138 contributions of agricultural management practices and environmental conditions on cropland  
139 N<sub>2</sub>O emission trends. This study considers direct emissions from croplands where synthetic  
140 fertilizers, livestock manure, human excreta, and crop residues are added, as well as indirect  
141 emissions due to atmospheric N deposition. Indirect emissions due to N leaching or runoff are  
142 not considered.

143

## 144 **2. Data and methods**

### 145 **2.1 Updated spatially-referenced nonlinear model (SRNM)**

146 The previous version of the SRNM model (Zhou et al., 2015) assume a quadratic relationship  
147 between cropland N application rates and N<sub>2</sub>O emissions, with spatially-variable model  
148 parameters depending on climate, soil properties, and crop management practices. The SRNM  
149 predict cropland-N<sub>2</sub>O emissions for each of geographical grids rather than administrative units.  
150 This calibrated formulation of N<sub>2</sub>O emissions was found to explain over 84% of the variance  
151 of field observations (Zhou et al., 2015), yet the model was only constrained by 732 field  
152 observations of N<sub>2</sub>O emissions. We updated the model by fitting the N<sub>2</sub>O emissions to new  
153 observations extended to 2,740 flux observations across 345 sites in the world (see Text S1,  
154 Tables S1~S2). The extended dataset covers a wider range of environmental conditions and  
155 agricultural management practices compared to our previous work and other similar studies  
156 (Gerber et al., 2016; Shcherbak et al., 2014) (Tables S3). The N<sub>2</sub>O emissions ( $E$ ) of the updated  
157 SRNM model is described as:

$$158 \quad E_{ijt} = \alpha_{ij} R_{ijt}^2 + \beta_{ij} R_{ijt} + \gamma_{ij} + \varepsilon_{ijt}, \quad (1a)$$

159 where

$$160 \quad \alpha_{ij} \sim N\left(X_k^T \lambda_{ijk}, \sigma_{ijk}^2\right), \beta_{ij} \sim N\left(X_k^T \phi_{ijk}, \sigma_{ijk}^2\right), \gamma_{ij} \sim N\left(X_k^T \varphi_{ijk}, \sigma_{ijk}^2\right), \quad (1b)$$

$$161 \quad \lambda_{ijk} \sim N\left(\mu_{ijk}, \omega_{ijk}^2\right), \phi_{ijk} \sim N\left(\mu'_{ijk}, \omega'_{ijk}{}^2\right), \varphi_{ijk} \sim N\left(\mu''_{ijk}, \omega''_{ijk}{}^2\right), \varepsilon_{ijt} \sim N\left(0, \tau^2\right), \quad (1c)$$

162 and  $i$  denotes the sub-function of N<sub>2</sub>O emissions ( $i=1, 2, \dots, I$ ).  $j$  represents the type of crop  
 163 ( $j=1-9$ , i.e., represents maize, wheat, paddy rice, vegetables, fruits, potatoes, oil crops, legume,  
 164 and the other crops).  $k$  is the index of climate factors or soil property ( $k=1-6$ , i.e., soil organic  
 165 carbon content, clay content, bulk density, soil pH, air temperature and the sum of precipitation  
 166 and irrigation).  $E_{ijt}$  denotes the N<sub>2</sub>O emission rate (kg N ha<sup>-1</sup> yr<sup>-1</sup>) predicted for crop type  $j$  in  
 167 year  $t$  in the  $i$ th type of regions.  $R_{ijt}$  is N application rate (kg N ha<sup>-1</sup> yr<sup>-1</sup>).  $\alpha$ ,  $\beta$ , and  $\gamma$  are  
 168 described as linear functions of climate or soil factors  $X_k$  (Table S2).  $\gamma$  is an intercept denoting  
 169 the background emission,  $\alpha R^2 + \beta R$  represents the fertilizer-induced emission,  $\alpha R + \beta$  being the  
 170 emission factor, and  $\varepsilon$  is the residual term. The random terms  $\lambda$ ,  $\phi$ ,  $\varphi$ , and  $\varepsilon$  are assumed to be  
 171 independent and normally distributed.  $\mu$  is the mean applied N effect for  $\alpha$  and  $\beta$  or the mean  
 172 emission baseline for  $\gamma$ .  $\sigma$ ,  $\omega$ , and  $\tau$  are standard deviations. All the parameter mean values and  
 173 standard deviations in each of sub-functions were estimated by the Bayesian Recursive  
 174 Regression Tree version 2 (BRRT v2) (Zhou et al., 2015), constrained by the extended dataset.  
 175 The estimated parameter values are presented in Table S4. The detailed methodology of the  
 176 BRRT v2 algorithm and the associated procedures can be found in Zhou et al. (2015).

177

## 178 2.2 New model inputs of N-fertilizers and irrigation

179 The updated SRNM model is forced by multiple gridded input datasets, including new datasets  
 180 describing N inputs and irrigation to croplands. For N inputs, we first collected nationwide  
 181 surveys of county-scale (the third-level administrative division) synthetic N fertilizer applied  
 182 to croplands ( $F_{SN}$ , kg N yr<sup>-1</sup>) for ~ 2900 counties in Mainland China, Taiwan, Hong Kong, and  
 183 Macau for the period 1990-2014. These data were further disaggregated by nine types of crop,

184 based on the crop-specific, provincial data of  $R_{ijt}$  from the Statistics of Cost and Income of  
185 Chinese Farm Produce (<http://tongji.cnki.net/overseas>). In addition, China has experienced  
186 changes of County-scale administrative divisions, such as aggregation, disaggregation, and  
187 name changes, so we harmonized the temporal evolution of  $F_{SN}$  to fit the latest administrative  
188 divisions (<http://geodata.pku.edu.cn>), based on the historical trajectories summarized by the  
189 Ministry of Civil Affairs of China (<http://xzqh.mca.gov.cn/>). More details can be found in Text  
190 S2. Second, we estimated annual N in livestock manure, human excreta, and crop residues  
191 returned to croplands by the *Eubolism* model at county scale (Chen, Chen, & Sun, 2010), based  
192 on county-scale activity data, such as the numbers of livestock by animal, rural population, and  
193 yields by crop type. The *Eubolism* model has been evaluated against multi-site observations in  
194 highly-fertilized cropping areas across China (see Text S3). Third, dry and wet deposition of  
195 N species were quantified by the global aerosol chemistry climate model LMDZ-OR-INCA at  
196 a horizontal resolution of 1.27° latitude by 2.5° longitude (Wang et al., 2017), in which wet N  
197 deposition fluxes have been validated by a recent global dataset (Vet et al., 2014). Finally, crop-  
198 specific N application rates ( $R_{ijt}$ ) were calculated as county-scale N input totals (i.e., synthetic  
199 fertilizers, manure, human excreta, crop residues, and N depositions) divided by the associated  
200 sowing areas that were obtained from the statistical yearbooks of 31 provinces  
201 (<http://tongji.cnki.net/overseas>). This new county-scale dataset of  $R_{ijt}$  was then resampled into  
202 a 1-km grid map based on the dynamic cropland distributions (Liu et al., 2014). We assumed  
203 a maximum N fertilizer application rate of 700 kg N ha<sup>-1</sup> based on a previous study (Carlson  
204 et al., 2017).

205

206 The second new gridded dataset is cropland irrigation application rate for the period 1990-2014.  
207 We first collected prefectural-level (i.e., the second-level administrative division) cropland  
208 irrigation amounts from two nationally-coordinated surveys: the 2<sup>nd</sup> National Water Resources

209 Assessment Program for the period 1990-2000 (China Renewable Energy Engineering Institute,  
210 2014) and the Water Resources Bulletins of 31 provinces for the rest of period 2001-2014  
211 ([www.mwr.gov.cn/english/pubs/](http://www.mwr.gov.cn/english/pubs/)). Both surveys had an identical methodology, including  
212 definitions, survey units, field surveys or measurements, and quality assurance. The detailed  
213 survey methodology is described in Text S4. It should be noted that cropland irrigation used  
214 here did not include water applied for aquaculture that accounts for less than 5% of agricultural  
215 irrigation (Zhu, Li, Li, Pan, & Shi, 2013). Cropland irrigation rates ( $\text{mm yr}^{-1}$ ) at the prefectural  
216 level were then calculated as cropland irrigation amounts divided by sowing areas. Similarly  
217 with  $R_{ijt}$ , these prefectural-scale cropland irrigation application rates were then disaggregated  
218 by resampling to 1-km gridded cropland maps for the period 1990-2014, and such rates were  
219 simply assumed same for each crop. Other data sources for model inputs can be found in Text  
220 S5, including soil properties and climate factors relevant to  $\text{N}_2\text{O}$  emissions.

221

### 222 **2.3 Model validation and comparison**

223 Process-based models were run using the same input data, and their outputs were compared  
224 with the results of the updated SRNM model. These process-based models include the Dynamic  
225 Land Ecosystem Model (DLEM) (Tian et al., 2015), the Organising Carbon and Hydrology In  
226 Dynamic Ecosystems (ORCHIDEE-OCN) (Zaehle & Friend, 2010), the Daily Century Model  
227 (DAYCENT) (Del Grosso et al., 2009), and Vegetation-Integrated Simulator for Trace Gases  
228 (VISIT) (Ito & Inatomi, 2012). Nitrification and denitrification processes in these models are  
229 expressed as functions of available substrates ( $\text{NH}_4^+$  or  $\text{NO}_3^-$  concentration), reaction rates,  
230 soil temperature and water content, but with different formulations and parameterizations (Tian  
231 et al., 2018). The results from atmospheric inversion of Saikawa et al. (2014), constrained by  
232 global measurements of  $\text{N}_2\text{O}$  atmospheric concentrations, were also compared with the  
233 estimated  $\text{N}_2\text{O}$  emissions. The new inversion was also conducted by replacing emissions from

234 this study for *a priori* agricultural soil emissions for China in the Bayesian inversion model  
235 (Saikawa et al., 2014). The detailed methodology and parameter calibration of the process-  
236 based models and the inversion model can be found in previous studies (Saikawa et al., 2014;  
237 Tian et al., 2018). In addition, the national estimates of cropland N<sub>2</sub>O emissions were compared  
238 with the state-of-the-art emission inventories, including the Food and Agriculture Organization  
239 Emission Database (FAOSTAT) (FAO, 2018), the Emissions Database for Global  
240 Atmospheric Research (EDGAR version 4.3.2) (Janssens-Maenhout et al., 2019), and the  
241 Greenhouse Gas and Air Pollution Interactions and Synergies (GAINS) (Winiwarter, Höglund-  
242 Isaksson, Klimont, Schöpp, & Amann, 2018), U.S. Environmental Protection Agency (USEPA)  
243 report (USEPA, 2012), and three China's National Communication Reports (CNCR; National  
244 Development and Reform Commission, 2017) submitted to the UNFCCC for years 1994, 2005,  
245 and 2012. Note that EDGAR, FAOSTAT and GAINS estimates were derived using the  
246 methodology of the 2006 IPCC Guidelines for National Greenhouse Gas Inventories (IPCC,  
247 2006) and national fertilizer data from the FAO.

248

#### 249 **2.4 Attribution of N<sub>2</sub>O emission trends**

250 We applied the Logarithmic Mean Divisia Index (LMDI) (Ang, 2015; Guan et al., 2018) to  
251 attribute N<sub>2</sub>O emission trends to different driving factors. The LMDI was chosen because of  
252 its path independence, consistency in aggregation, and ability to handle zero values (Ang,  
253 2015). The LMDI analysis compares a set of driving factors between the base and final year of  
254 a given period, and explores the effects of these factors on the change in China's cropland-N<sub>2</sub>O  
255 emissions over that period. The detailed methodology of LMDI can be found in Ang (2015).  
256 According to previous modeling studies (Guan et al., 2018), we decomposed cropland-N<sub>2</sub>O  
257 emissions into a combination of different drivers: total sowing area ( $A_k$ , ha), the share of nine  
258 different crops to total sowing area ( $m_{jk}$ , %) also known as crop mix, N application rate ( $R_{jk}$ , kg

259 N ha<sup>-1</sup> yr<sup>-1</sup>), and the emission intensity ( $e_{jk}$ , %) per crop type and region:

$$260 \quad E_k = \sum_j \left( A_k \times \frac{A_{jk}}{A_k} \times \frac{N_{jk}}{A_{jk}} \times \frac{E_{jk}}{N_{jk}} \right) = \sum_j (A_k \times m_{jk} \times R_{jk} \times e_{jk}), \quad (2)$$

261 where region  $k=1-8$  corresponds to China, the Northwest, the Northeast Plain, the North China  
 262 Plain, the lower reach of Yangtze River basin, the Southwest, the Northwest, and Qinghai-  
 263 Tibet Plateau;  $A_{jk}$  is the sowing area of crop  $j$  in cropping region  $k$ ;  $N_{jk}$  and  $E_{jk}$  are N-fertilizer  
 264 application amount and croplands N<sub>2</sub>O emission of crop  $j$  in cropping region  $k$ , respectively. It  
 265 should be noted that  $e_{jk}$  is defined as cropland-N<sub>2</sub>O emission per unit of  $N_{jk}$ , which is different  
 266 from the emission factor defined in the 2006 IPCC Guidelines, and represents the gross  
 267 emission intensity at a given N application level. The change of  $E$  of region  $k$  in the year  $t$   
 268 compared to the year  $t - 1$  is computed as

$$269 \quad \Delta E_k = \sum_j w_{jk} \ln \left( \frac{A_k^t}{A_k^{t-1}} \right) + \sum_j w_{jk} \ln \left( \frac{a_{jk}^t}{a_{jk}^{t-1}} \right) + \sum_j w_{jk} \ln \left( \frac{R_{jk}^t}{R_{jk}^{t-1}} \right) + \sum_j w_{jk} \ln \left( \frac{e_{jk}^t}{e_{jk}^{t-1}} \right). \quad (3)$$

$$= \Delta E_A + \Delta E_m + \Delta E_R + \Delta E_e$$

270 Here,  $w_{jk} = (E_{jk}^t - E_{jk}^{t-1}) / (\ln E_{jk}^t - \ln E_{jk}^{t-1})$  is a weighting factor called the logarithmic mean  
 271 weight (Ang, 2015).  $\Delta E_A$ ,  $\Delta E_m$ ,  $\Delta E_R$ , and  $\Delta E_e$ , are changes in  $E$ , corresponding to change in  
 272 total sowing area, shift in crop mix, change in N application rate, and emission intensity,  
 273 respectively. The change of  $\Delta E$  between base and final years is then calculated by the  
 274 cumulative  $\Delta E$  between adjacent years. The sign of the  $\Delta E$  indicates a positive or negative  
 275 effect of the factor on the change of cropland N<sub>2</sub>O emissions between the base and final years,  
 276 and the potential impacts of nationwide policy interventions related to fertilizer application,  
 277 crop type and sowing area.

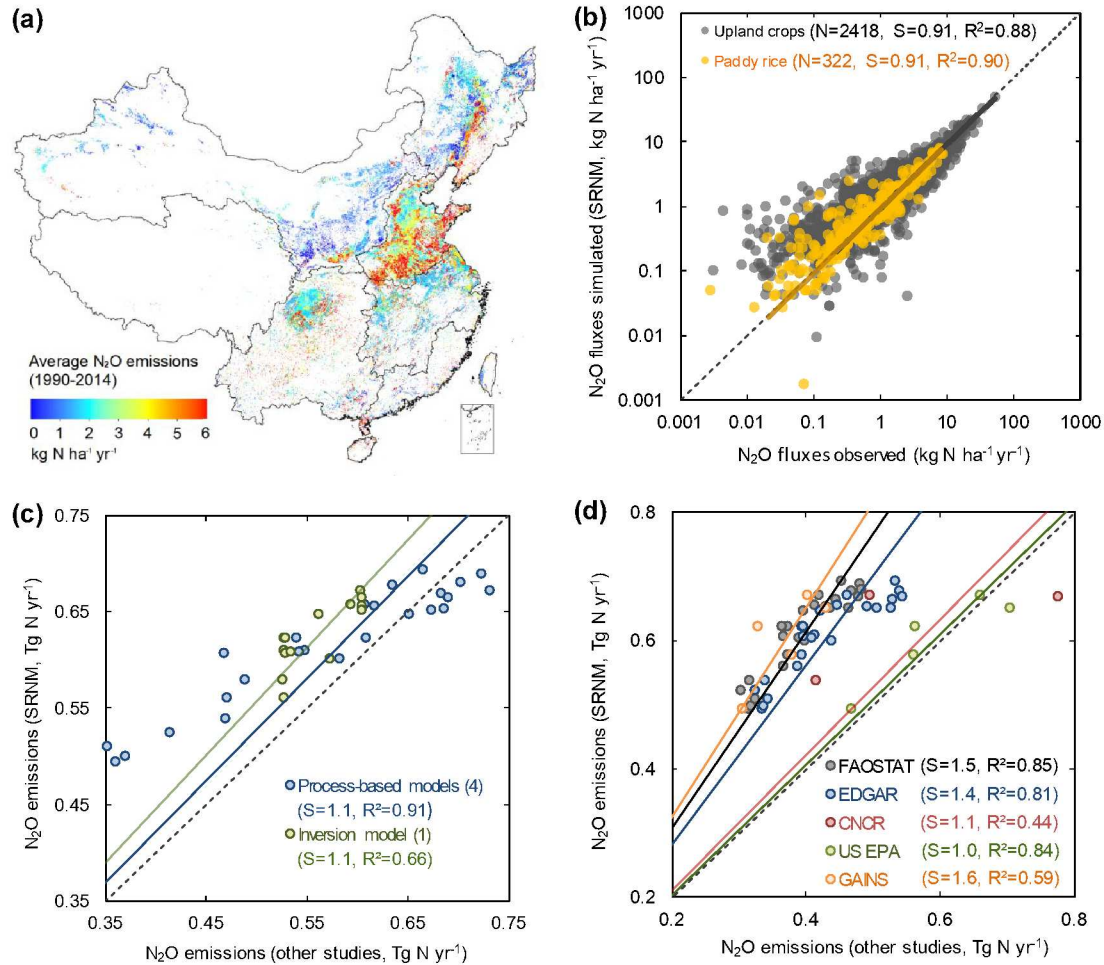
278

## 279 **3. Results**

### 280 **3.1 Model performance**

281 Combining the new N inputs and irrigation data and the other forcing datasets with the updated  
282 SRNM model, we estimated a mean annual N<sub>2</sub>O emission from China's croplands of  $0.62 \pm$   
283  $0.06 \text{ Tg N yr}^{-1}$  during the period 1990-2014 (one standard deviation due to inter-annual  
284 variability of N<sub>2</sub>O emissions), with the spatial distribution shown in Fig. 1a. The validity of  
285 our N<sub>2</sub>O emission estimates was supported by internal cross-validation at 345 sites ( $R^2=0.88$   
286 and 0.90 for upland crops and paddy rice, respectively, Fig. 1b). In addition, our SRNM model  
287 outputs performed well in reproducing the spatial contrast and long-term inter-annual  
288 variability of N<sub>2</sub>O emissions as well as the sensitivity of N<sub>2</sub>O emission to environmental  
289 changes (Figs S1 and S2). In addition, the N<sub>2</sub>O emissions were corroborated against  
290 independent simulations from four process-based models and the estimates from the  
291 atmospheric inversion ( $R^2 = 0.91$  and  $0.66$ , respectively, Fig. 1c). This new estimate of China's  
292 cropland N<sub>2</sub>O emissions is consistent with the USEPA report ( $0.59 \text{ Tg N yr}^{-1}$ ) (USEPA, 2012),  
293 and in general fell with the range of process-based models ( $0.35$  to  $0.73 \text{ Tg N yr}^{-1}$ , Fig. 1c).  
294 However, it exceeded emission estimates provided by EDGAR v4.3.2 product (Janssens-  
295 Maenhout et al., 2017) by 43%, the FAOSTAT by +55%, the GAINS by 67%, and the CNCR  
296 for years 1994 and 2005 by 36% (*t*-test at the 95% level, Fig. 1d), but was comparable to the  
297 latest CNCR report for the year 2012 ( $0.78 \text{ Tg N yr}^{-1}$ ).

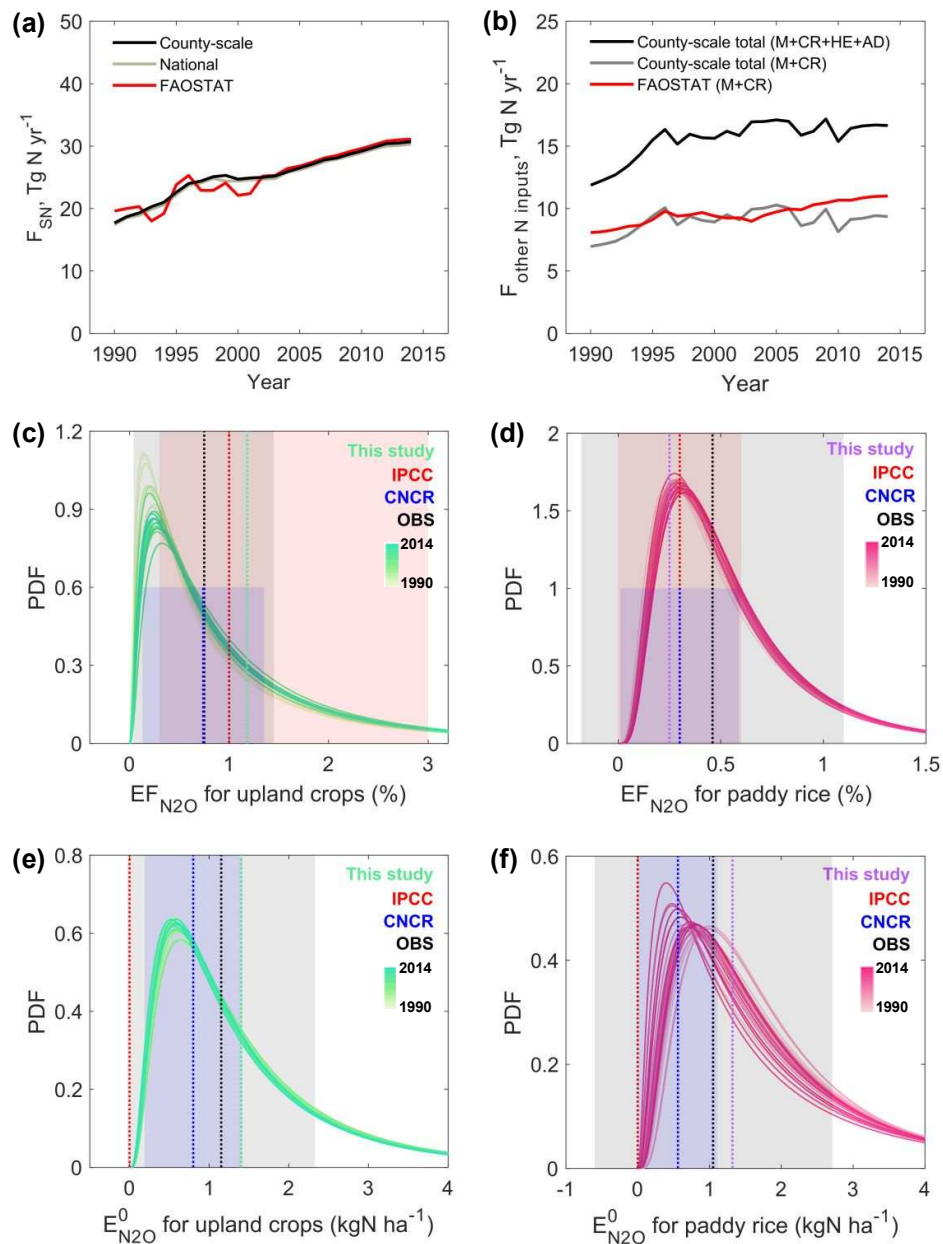
298



299

300 **Figure 1. Validation of China's cropland  $N_2O$  emissions from the updated SRNM model.**  
 301 (a) Pattern of mean annual  $N_2O$  emissions simulated (1990-2014). (b) Model performance of  
 302 the simulated cropland  $N_2O$  fluxes. (c) Comparison of annual cropland  $N_2O$  emissions against  
 303 the means of process-based models (1990-2014) and inversion models (1996-2008). Each point  
 304 represents the estimated  $N_2O$  emissions from Chinese croplands for a certain year. Numbers in  
 305 brackets show the number of models. (d) Comparison of annual cropland  $N_2O$  emissions with  
 306 the emission inventories, including FAOSTAT (1990-2014), EDGAR v4.3.2 (1990-2012),  
 307 CNCR (1994, 2005, 2012); USEPA (1990-2005), and GAINS (1990, 1995, 2000, 2005, 2010).  
 308 Note that N, S, and  $R^2$  denote the number of measurements, slope of regression line, and  
 309 coefficient of determination, respectively.





310

311 **Figure 2. Comparisons of N inputs, emission factor and ‘background’ anthropogenic**  
 312 **emissions of cropland N<sub>2</sub>O in China. (a) Synthetic fertilizers applied to croplands. (b)**  
 313 **N inputs, including manure (M), crop residues (CR), human excreta (HE) returned to croplands,**  
 314 **and atmospheric deposition (AD) over croplands. (c) Lognormal probability density function**  
 315 **of emission factor for all upland crops based on gridded results during the period 1990-2014,**  
 316 **where the dashed lines indicate the median values, and shaded areas represent standard**  
 317 **deviation for this study and observed values (OBS) or 95% confidence interval for the IPCC**  
 318 **and the CNCR. (d) Same as panel c but for paddy rice. (e) Same as panel c but for background**  
 319 **emission (E<sup>0</sup>) of upland rice. (d) Same as panel c but for E<sup>0</sup> of paddy rice. Note that the**  
 320 **definition of FAOSTAT, IPCC, CNCR, and OBS can be found in the text.**

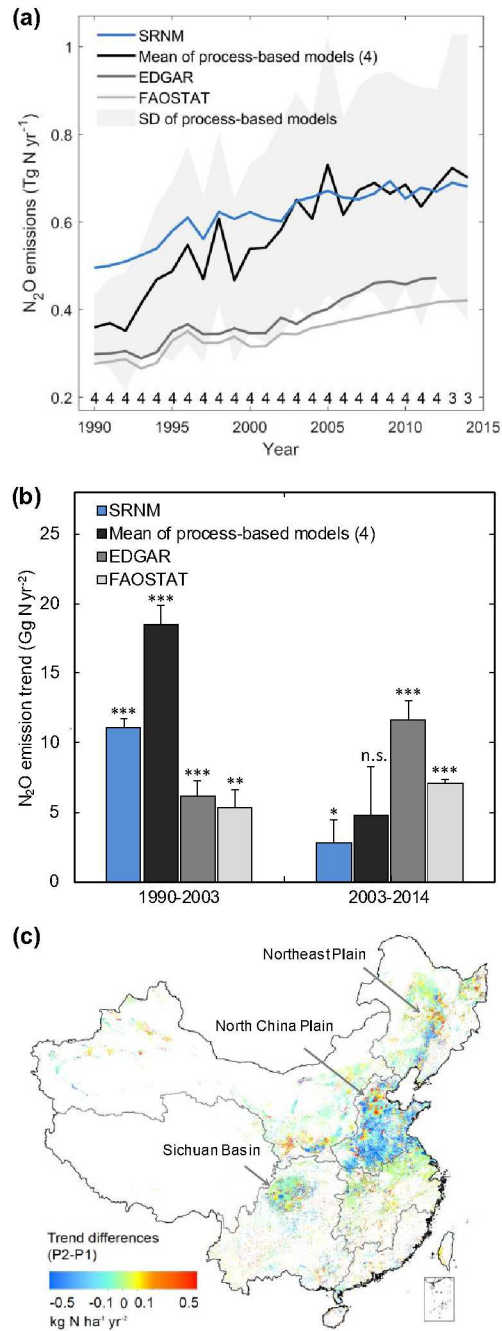
321

322 The differences between our estimates and other inventories were primarily attributed to the  
323 updates of N input data, emission factors, and ‘background’ anthropogenic emissions from soil  
324 residual N (Fig. 2). First, our county-scale estimation of synthetic N fertilizer application was  
325 almost identical to the national statistics and FAOSTAT data (Fig. 2a), whereas the other N  
326 inputs were substantially larger because the inclusion of human excretion and atmospheric  
327 deposition over croplands (Figs 2b and S3). Second, our estimate of the nationally-averaged  
328 N<sub>2</sub>O emission factor (EF) for upland crops was larger than IPCC Tier 1 default by 20% (Fig.  
329 2c), but the EF was -17% lower for paddy rice (Fig. 2d and Text S6). Furthermore, the  
330 ‘background’ anthropogenic emissions of N<sub>2</sub>O ( $\gamma$ ) due to the legacy effect resulting from  
331 historical soil N accumulation were estimated to be  $1.40 \pm 0.04$  kg N ha<sup>-1</sup> yr<sup>-1</sup> for upland crops  
332 and  $1.30 \pm 0.05$  kg N ha<sup>-1</sup> yr<sup>-1</sup> for paddy rice in this study (Figs 2e and 2f), while they were not  
333 fully accounted for by the IPCC Tier 1 inventories. Our estimates of this term were larger than  
334 the values used in the CNCR (0.80 and 0.56 kg N ha<sup>-1</sup> yr<sup>-1</sup>), but generally agreed with the *in*  
335 *situ* observations (OBS) with zero N input ( $1.2 \pm 1.2$  and  $1.0 \pm 1.7$  kg N ha<sup>-1</sup> yr<sup>-1</sup> based on 168  
336 and 54 sites, respectively).

337

### 338 **3.2 Trend in cropland N<sub>2</sub>O emissions in China**

339 Over the period 1990-2014, cropland N<sub>2</sub>O emissions showed a persistent and widespread  
340 increase (Fig. S4), because of the significant increase in N inputs to croplands. However, the  
341 rate of this increase slowed down from 11.2 Gg N yr<sup>-2</sup> ( $P < 0.001$ ) before 2003 to 2.8 Gg N  
342 yr<sup>-2</sup> ( $P = 0.02$ ) afterwards (Figs 3a and 3b), a turning point detected by Pettitt's test (Pettitt,  
343 1979) ( $P < 0.001$ ). This slower, insignificant growth of cropland-N<sub>2</sub>O emissions was confirmed  
344 by the process-based models with the same forcing datasets (19.8 Gg N yr<sup>-2</sup> for 1990-2003,  $P$   
345  $< 0.001$ ; 4.8 Gg N yr<sup>-2</sup> for 2003-2014,  $P = 0.15$ ; Fig. 3b). We then divided the past 25 years  
346 into two periods covering 1990-2003 (P1) and 2003-2014 (P2). Regionally,



347

348 **Figure 3. The inter-annual variability of cropland-N<sub>2</sub>O emissions in China.** (a) Temporal  
 349 evolution of annual cropland-N<sub>2</sub>O emissions based on the updated SRNM model, an ensemble  
 350 of four process-based models, and previous inventories (EDGAR v4.3.2 and FAOSTAT).  
 351 Shaded area indicates the standard deviation of the results from process-based models.  
 352 Numbers at the bottom show the number of process-based models available for each year. (b)  
 353 Trends in cropland-N<sub>2</sub>O emissions based on different approaches for two different periods (P1:  
 354 1990-2003, P2: 2003-2014); \*\*\*, \*\*, and \* indicate significance of the trends at the 99.9%, 99%  
 355 and 95% confidence interval, respectively; n.s., not significant. (c) Pattern of the difference in  
 356 N<sub>2</sub>O trends between the two periods.

357 approximately 64% of the Chinese sowing area experienced a weakened growth or even a  
358 decline of N<sub>2</sub>O emissions in P2, primarily located in major cropping areas such as the North  
359 China Plain, the Sichuan Basin, and a part of the Northeast Plain (Fig. 3c), while the rest  
360 showed a growth in emissions, mainly in Heilongjiang province and the Northwest China (Fig.  
361 3c). By contrast, the estimates provided by EDGAR v4.3.2 have suggested enhanced growth  
362 of cropland-N<sub>2</sub>O emissions across China (Figs 3b and S5). The estimated growth rate of  
363 cropland-N<sub>2</sub>O emissions in EDGAR v4.3.2 after 2003 (11.6 Gg N yr<sup>-2</sup>,  $P < 0.001$ ) is much  
364 larger than that for 1990-2003 (6.2 Gg N yr<sup>-2</sup>,  $P < 0.001$ ; Fig. 3b). Differences in emission  
365 trends between our estimates and the EDGAR product are mainly focused around the North  
366 China Plain (Fig. S5).

367

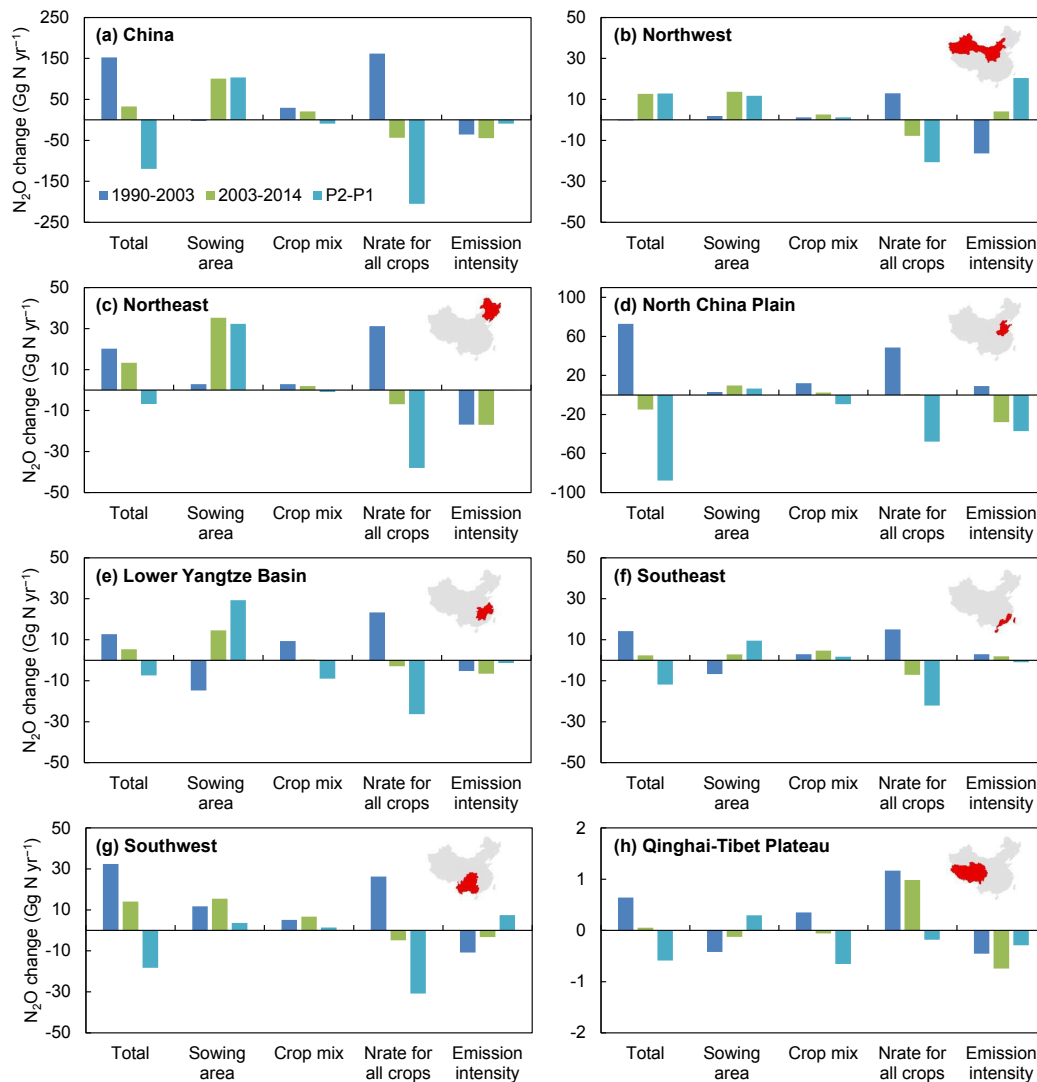
### 368 **3.3 Drivers of China's cropland-N<sub>2</sub>O emission trends**

369 The decomposition analysis in Fig. 4 shows the contribution of each of the four drivers to the  
370 change in cropland-N<sub>2</sub>O emissions in China and its seven major cropping regions. For P1, the  
371 trend of emissions was associated with a growth of N<sub>rate</sub> for all crops (Fig. 4a), mainly located  
372 in the North China Plain and the Northeast Plain (Figs 4c-4d). For P2, the slower growth in  
373 cropland-N<sub>2</sub>O emissions across China was driven by the downward influences from the  
374 reduced N<sub>rate</sub> and emission intensities, which largely offset the strong expansion of sowing  
375 areas particularly in the Northeast Plain (Figs 4a and 4c). By contrast, the shifts in the crop mix  
376 and in emission intensity contributed marginally to changes in emissions in both periods (Fig.  
377 4a).

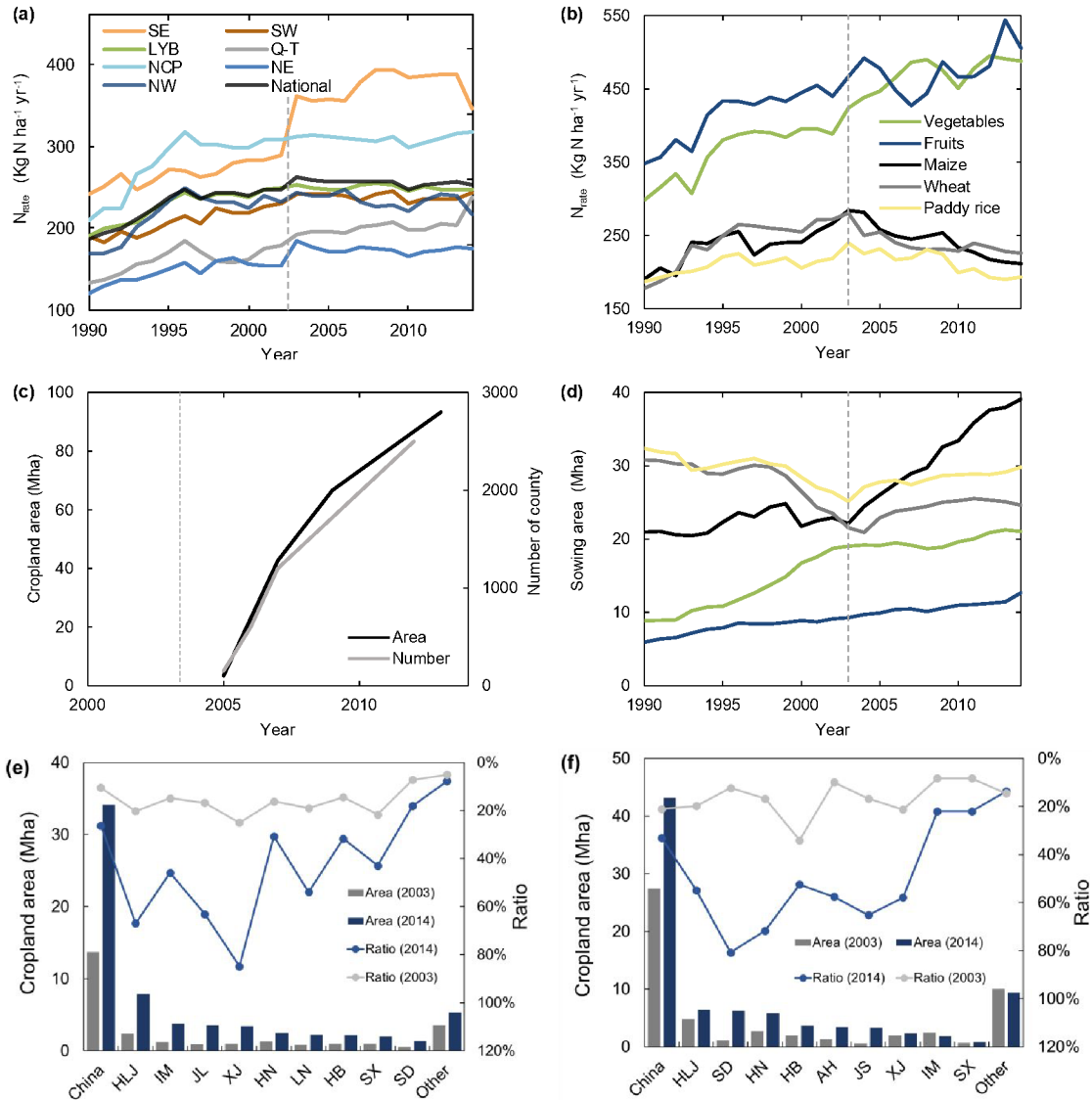
378

379 Contributions of the four driving factors to cropland-N<sub>2</sub>O emission trends differed between  
380 cropping regions (Figs 4b-4h). During the period P1, the trend in cropland-N<sub>2</sub>O emissions was  
381 explained by the growth of N<sub>rate</sub> in most of the major cropping regions, except for the Northwest

382 where there was decreased emission intensity. During the period P2, sowing area expansion  
 383 became the largest contributor to the positive cropland-N<sub>2</sub>O emission trends in the Northeast  
 384 Plain, the Northwest, the Southwest, as well as the lower reaches of the Yangtze River basin.  
 385 However, the decrease in emission intensity dominated the change in cropland-N<sub>2</sub>O emissions  
 386 in the North China Plain, and N<sub>rate</sub> contributed to the changes in the Southeast and Qinghai-  
 387 Tibet Plateau.



388 **Figure 4. Contribution of different drivers to the change in cropland-N<sub>2</sub>O emissions by**  
 389 **cropping region during 1990-2003 (P1) and 2003-2014 (P2).** a. China; b. northwest China;  
 391 c. northeast China; d. North China Plain; e. lower Yangtze Basin; f. southeast China; g.  
 392 southwest China; h. Qinghai-Tibet Plateau. Note varying vertical-axes. The length of each bar  
 393 reflects the contribution of each factor during the corresponding period.



394

395

396 **Figure 5. Temporal evolution of agricultural management in China. a.**  $N_{rate}$  in 7 major397 cropping regions. **b.**  $N_{rate}$  by crops. **c.** National sowing areas and county number applied by the398 Nationwide Soil Testing and Formulation Fertilization Program. **d.** National sowing areas by399 crops. **e.** Provincial areas and ratio of croplands using mechanically-aided deep placement of

400 fertilizers in 2003 and 2014, where the ratio is calculated as the croplands using this technology

401 divided by national cropland area. **f.** Same as panel e but for crop residues returned to croplands.

402 The seven cropping regions include Southeast (SE), Southwest (SW), Lower Yangtze Basin

403 (LYB), Qinghai-Tibet Plateau (Q-T), North China Plain (NCP), Northeast (NE) and Northwest

404 (NW). HLJ: Heilongjiang, IM: Inner Mongolia, JL: Jilin, XJ: Xinjiang, HN: Henan, LN:

405 Liaoning, HB: Hebei, SX: Shanxi, SD: Shandong, AH: Anhui, JS: Jiangsu

406 Overall, in period P2 (after 2003), the reduction of  $N_{rate}$  dominated the slowdown of cropland-407  $N_2O$  emissions in China. According to nationwide statistics, China's  $N_{rate}$  showed a clear

408 reversal in trend around 2003, from an increasing rate of  $+5.1 \text{ kg N ha}^{-1} \text{ yr}^{-2}$  in P1 to a decrease  
409 of  $-0.7 \text{ kg N ha}^{-1} \text{ yr}^{-2}$  in P2, although it varied across different cropping regions (Fig. 5a).  
410 Similar decreases in crop-specific  $N_{\text{rate}}$  were found for wheat, maize, and paddy rice, but not  
411 for vegetables and fruits, all with Pettitt's test (Fig. 5b,  $p < 0.001$ ). Interestingly, these change  
412 points were, in general, coincident with changes in cropland- $\text{N}_2\text{O}$  emissions in China. The  
413 reductions of  $N_{\text{rate}}$  were mainly due to declines in synthetic fertilizer uses, particularly in the  
414 eastern and central China, the Yunnan-Guizhou Plateau, and the North China Plain (Fig. S6).

415

#### 416 **4. Discussion**

417 Reliable estimation of cropland- $\text{N}_2\text{O}$  emissions and their drivers is fundamental to the  
418 development of policy for sustainable N management. Previous estimates have shown large  
419 differences in the magnitude and temporal evolution of annual cropland- $\text{N}_2\text{O}$  emissions. This  
420 has mainly been due to the lack of high-resolution data on agricultural management and of  
421 spatial representation in the models. Our updated SRNM model, along with new, crop-specific  
422 gridded datasets of N inputs and irrigation, permits a new insight into the spatial contrast and  
423 inter-annual variability of cropland- $\text{N}_2\text{O}$  emissions, and associates these with policy-driven  
424 technological adoption and environmental changes.

425

426 The reduced  $N_{\text{rate}}$  suggests that national N use efficiency of fertilizers has improved over recent  
427 decades, given that there was no reduction in per-area crop yields according to the national  
428 statistics (Sun & Huang, 2012). One of the most effective methods of making fertilizer use  
429 more efficient is to match the supply of nutrients with demand during field application  
430 (Richards et al., 2015). Such an approach was one of targets of the Nationwide Soil Testing  
431 and Formulation Fertilization Program, launched in the early 2000s (Table S7). This program  
432 started with staple crops, which account for  $\sim 50\%$  of national N inputs on average, but after

433 2010 it extended to a number of cash crops. These improved N use efficiencies for staple crops  
434 were also found in the most recent study (Zou et al., 2018). According to national statistics  
435 (Sun & Huang, 2012), such technologies increased in prevalence on croplands from 3.3 million  
436 ha in 200 counties, to ~93 million ha in 2,498 counties (Fig. 5c). In addition, spatial re-  
437 allocation of crops has extensively happened in China over recent decades, and is characterized  
438 by an emerging shift from peri-urban areas in the South and Central China (high N rate) to rural  
439 areas in the North (low N rate) because of urbanization (Fig. S7; Zou et al., 2018). Although  
440 the effectiveness of the Nationwide Soil Testing and Formulation Fertilization Program on the  
441  $N_{\text{rate}}$  is difficult to quantify at the regional scale, these measures contributed to the decline in  
442  $N_{\text{rate}}$  across China (Chen et al., 2014).

443

444 The increased sowing area was identified as the second important driver of cropland- $N_2O$   
445 emission trends in P2 that partially offset the effect of decreasing  $N_{\text{rate}}$ . The shift in crop mix  
446 resulted in positive emission trends in P1, but made negligible contributions across most  
447 cropping regions in P2. Specifically, sowing areas by crop have changed in line with multiple  
448 nationwide crop structural transition programs in China. During the period 1990-2003, the  
449 Government of China encouraged the growth of cash crops to meet increased consumption  
450 requirements. According to national statistics, the sowing areas of vegetables and fruits  
451 increased by 115% and 57% in the P1 (Fig. 5d), respectively. Meanwhile, the areas sown to  
452 wheat and paddy rice declined by -30% and -22%, and sowing area of maize remained at the  
453 level as that in 1990. This structural transition in cropping patterns that occurred in P1 resulted  
454 in more cropland- $N_2O$  emissions, because vegetables and fruits, which constitute the major  
455 area of cash crops, have an emission factor two times higher than that of staple crops (Dobbie  
456 & Smith, 2003). During P2 (after 2003), the Government of China aimed to stabilize the  
457 production of cash crops, but to also restore the production of cereal crops. As a result, the



458 sowing areas of staple crops increased by 36%, while the sowing areas of vegetables, fruits,  
459 and oil crops were increased by only 11% (Fig. 5d). Compared to the period P1, this shift in  
460 crop mix in P2 exerted a lower upward pressure on cropland-N<sub>2</sub>O emissions, particularly in the  
461 major cropping regions. The results underscore the significance of land-use changes to the  
462 spatial and inter-annual variabilities of N<sub>2</sub>O emissions.

463

464 Our results show that emission intensity decreased during both periods and had a negative  
465 effect on the growth of cropland-N<sub>2</sub>O emissions across most of the cropping regions. Scenario  
466 simulations based on the SRNM (see Text S7) suggest that N<sub>rate</sub> was the dominant factor  
467 controlling the emission intensity trend, followed by soil organic carbon (SOC) and water  
468 inputs (Fig. S8). Increased SOC offset 19% and 51% of the negative effects from N<sub>rate</sub> for P1  
469 and P2, respectively. Thus whilst C sequestration can help offset some of the cropland  
470 emissions of CO<sub>2</sub>, a recent study suggests that carbon emission equivalents of non-CO<sub>2</sub> GHG  
471 emissions are currently ~12 times greater than carbon uptake by Chinese croplands over 100-  
472 year time horizon (B. Gao et al., 2018). SOC also played a role in increasing N<sub>2</sub>O emissions  
473 with a positive correlation between N<sub>2</sub>O emissions and SOC reported in field (Figueiredo,  
474 Enrich - Prast, & Rütting, 2016), laboratory studies (Jäger, Stange, Ludwig, & Flessa, 2011),  
475 meta-analyses (Bouwman, Boumans, & Batjes, 2002; Charles et al., 2017), and data mining  
476 analysis (Perlman et al., 2014). The positive effect of SOC could be explained by high SOC  
477 providing sources of energy, C and N for nitrifying and denitrifying microorganisms, and  
478 creating anaerobic conditions favoring the oxidation-reduction reaction for denitrification  
479 (Charles et al., 2017).

480

481 At present, the attribution of trends in cropland-N<sub>2</sub>O emissions to driving factors contains some  
482 uncertainties. Other potential factors responsible for the decline in emissions seem also to be

483 important, but were difficult to consider explicitly. These include, among others, changes in  
484 crop cultivars (Zhang, Fan, Wang, & Shen, 2009), cultivation technology improvements places  
485 (Jiang et al., 2018), timing (Jiang et al., 2018; Wang et al., 2016) and placement methods (Chen,  
486 Wang, Liu, Lu, & Zhou, 2016), and changes in fertilizer type (Bouwman et al., 2002). For  
487 example, multiple field trials for staple crops in China suggest a significant increase in N-use  
488 efficiency (ratio of yield to  $N_{\text{rate}}$ ) associated with cultivar improvement over recent decades (de  
489 Dorlodot et al., 2007). However, this does not mean a coincident reduction of  $N_{\text{rate}}$  because  
490 crop yields (i.e., per-area crop production of these new cultivars) grew synergistically, and thus  
491 might require more fertilizer per unit of cropped area. The improvement of cultivation  
492 technology plays an important role in influencing cropland- $N_2O$  emissions. For example, the  
493 proportion of croplands using mechanically-aided deep placement of fertilizers increased from  
494 11% in 2003 to 26% at present, particularly in the north of China (Fig. 5e), decreasing the N  
495 losses and thereby cropland- $N_2O$  emissions. Increasing the return of crop residues, also  
496 particularly in the North China Plain, has been hypothesized as an emerging driver for the  
497 change of  $N_{\text{rate}}$ . In these regions, crop residues returned to croplands accounted for from 21%  
498 in 2003 to 33% of croplands in 2014 (Fig. 5f), increasing the potential to replace the application  
499 of synthetic fertilizers, and to change carbon and N biogeochemical cycles in soils (Chen, Li,  
500 Hu, & Shi, 2013; Xia et al., 2018). However, the effect of crop residues on cropland- $N_2O$   
501 emissions is more complex and modified by the prevalence of aerobic and anaerobic soil  
502 conditions (Xia et al., 2018), and also the chemical composition of the plant material (S. Gao  
503 et al., 2018).

504

505 In summary, the results from this study underline the advantage of high-resolution agricultural  
506 activity data and emission intensity detailed by crop type, land-use dynamics and technology  
507 improvement to understand the change in cropland- $N_2O$  emissions. Most of the state-of-the-art

508 emission inventories that aim to quantify global N<sub>2</sub>O emissions, fail to capture either the  
509 magnitude or temporal trends in China. This is because firstly, an IPCC default EF of 1%  
510 assumes a constant relationship between N input and N<sub>2</sub>O emissions. This cannot reproduce  
511 the spatial and temporal responses of N<sub>2</sub>O emission to environmental changes. Secondly,  
512 emission inventories, in general, disaggregate national-scale or low-resolution fertilizer and  
513 irrigation data into gridded maps to generate cropland-N<sub>2</sub>O emission patterns. This would be  
514 likely to lower emission estimates from regions predominantly fertilized at high N inputs (e.g.,  
515 the North China Plain), while increasing emission estimates from under-fertilized areas (e.g.,  
516 the Northeast Plain). Process-based terrestrial biosphere models (TBM) still face many  
517 challenges in modelling changes in cropland-N<sub>2</sub>O emissions (Sandor et al. 2018). Though most  
518 of them consider the biotic and abiotic processes involved N<sub>2</sub>O production, they also generate  
519 divergent estimates of cropland-N<sub>2</sub>O emissions and spatio-temporal patterns (Tian et al., 2018).  
520 Possible reasons for divergent estimates among TBMs are the incomplete model representation  
521 of N<sub>2</sub>O emissions in response to agricultural management practices and uniform response  
522 functions of the N<sub>2</sub>O flux to environmental conditions (e.g., SOC). Improving the  
523 representation of crop-specific agricultural activity data and the regional adoptions of N<sub>2</sub>O flux  
524 response are recommended for future projections.

525

526 The updated SRNM model for China's cropland-N<sub>2</sub>O emissions could be extended to other  
527 countries for updating their cumulative emissions and their contributions to global historical  
528 radiative forcing and ozone depletion. The decomposition of cropland-N<sub>2</sub>O emission trends to  
529 underlying drivers could facilitate the tracking of key indicators that require significant change.  
530 Our modeling results also highlight that technological adoption was intertwined with policy  
531 interventions in China. We argue that designing more realistic future scenarios for  
532 technological adoption will increase the likelihood that policies will be implemented to set

533 targets and incentives for cropland-N<sub>2</sub>O emission mitigation.

534

## 535 **ACKNOWLEDGMENT**

536 This study was supported by the National Natural Science Foundation of China (41671464;  
537 7181101181), the National Key Research and Development Program of China  
538 (2016YFD0800501; 2018YFC0213304), 111 Project (B14001), the GCP-INI Global N<sub>2</sub>O  
539 Budget and the INMS Asia Demo Activities. The input of P.S. contributes to the UK-China  
540 Virtual Joint Centre on Nitrogen “N-Circle” funded by the Newton Fund *via* UK  
541 BBSRC/NERC (BB/N013484/1). We acknowledged Eric Ceschia, Kristiina Regina, Dario  
542 Papale, and the NANORP for sharing a part of observation data.

543

## 544 **REFERENCES**

- 545 Alexandratos, N., & Bruinsma, J. (2012). *World agriculture towards 2015/2030: The 2012*  
546 *Revision. ESA Working Paper* (Vol. 12, No. 3). FAO, Roma.  
547 [https://doi.org/10.1016/S0264-8377\(03\)00047-4](https://doi.org/10.1016/S0264-8377(03)00047-4)
- 548 Allen, M. R., Coninck, H. D., Connors, S., Engelbrecht, F., Ferrat, M., Ford, J., ... Taylor, M.  
549 IPCC Special Report on Global Warming of 1.5°C. In Press.
- 550 Ang, B. W. (2015). LMDI decomposition approach: A guide for implementation. *Energy*  
551 *Policy*, 86, 233–238. <https://doi.org/10.1016/j.enpol.2015.07.007>
- 552 Bouwman, A. F., Boumans, L. J. M., & Batjes, N. H. (2002). Emissions of N<sub>2</sub>O and NO from  
553 fertilized fields: Summary of available measurement data. *Global Biogeochemical Cycles*,  
554 16(4), 6-1-6–13. <https://doi.org/10.1029/2001GB001811>
- 555 Carlson, K. M., Gerber, J. S., Mueller, N. D., Herrero, M., MacDonald, G. K., Brauman, K. A.,  
556 ... West, P. C. (2017). Greenhouse gas emissions intensity of global croplands. *Nature*

- 557 *Climate Change*, 7(1), 63–68. <https://doi.org/10.1038/nclimate3158>
- 558 Charles, A., Rochette, P., Whalen, J. K., Angers, D. A., Chantigny, M. H., & Bertrand, N.  
559 (2017). Global nitrous oxide emission factors from agricultural soils after addition of  
560 organic amendments: A meta-analysis. *Agriculture, Ecosystems and Environment*, 236,  
561 88–98. <https://doi.org/10.1016/j.agee.2016.11.021>
- 562 Chen, H., Li, X., Hu, F., & Shi, W. (2013). Soil nitrous oxide emissions following crop residue  
563 addition: A meta-analysis. *Global Change Biology*, 19(10), 2956–2964.  
564 <https://doi.org/10.1111/gcb.12274>
- 565 Chen, M., Chen, J., & Sun, F. (2010). Estimating nutrient releases from agriculture in China:  
566 An extended substance flow analysis framework and a modeling tool. *Science of the Total*  
567 *Environment*, 408(21), 5123–5136. <https://doi.org/10.1016/j.scitotenv.2010.07.030>
- 568 Chen, X., Cui, Z., Fan, M., Vitousek, P., Zhao, M., Ma, W., ... Zhang, F. (2014). Producing  
569 more grain with lower environmental costs. *Nature*, 514(7523), 486–489.  
570 <https://doi.org/10.1038/nature13609>
- 571 Chen, Z., Wang, H., Liu, X., Lu, D., & Zhou, J. (2016). The fates of <sup>15</sup>N-labeled fertilizer in a  
572 wheat–soil system as influenced by fertilization practice in a loamy soil. *Scientific Reports*,  
573 6, 34754. Retrieved from <https://doi.org/10.1038/srep34754>
- 574 China Renewable Energy Engineering Institute. (2014). *Evaluation of China's water resources*  
575 *and its exploitation and utilization*. Beijing: China Water & Power Press.
- 576 National Development and Reform Commission (NDRC) (2017). *The People's Republic of*  
577 *China first biennial update report on climate change*. Retrieved from  
578 <http://qhs.ndrc.gov.cn/dtjj/201701/W020170123346264208002.pdf>
- 579 de Dorlodot, S., Forster, B., Pagès, L., Price, A., Tuberosa, R., & Draye, X. (2007). Root  
580 system architecture: opportunities and constraints for genetic improvement of crops.  
581 *Trends in Plant Science*, 12(10), 474–481. <https://doi.org/10.1016/j.tplants.2007.08.012>

- 582 Del Grosso, S. J., Ojima, D. S., Parton, W. J., Stehfest, E., Heistemann, M., DeAngelo, B., &  
583 Rose, S. (2009). Global scale DAYCENT model analysis of greenhouse gas emissions  
584 and mitigation strategies for cropped soils. *Global and Planetary Change*, *67*, 44–50.  
585 <https://doi.org/10.1016/j.gloplacha.2008.12.006>
- 586 Dobbie, K. E. , & Smith, K. A. (2003). Nitrous oxide emission factors for agricultural soils in  
587 Great Britain: the impact of soil water-filled pore space and other controlling variables.  
588 *Global Change Biology*, *9*(2), 204-218. <https://doi.org/10.1046/j.1365-2486.2003.00563.x>
- 589 Ehrhardt, F., Soussana, J. F., Bellocchi, G., Grace, P., McAuliffe, R., Recous, S., ... & Basso,  
590 B. (2018). Assessing uncertainties in crop and pasture ensemble model simulations of  
591 productivity and N<sub>2</sub>O emissions. *Global Change Biology*, *24*(2), 603-616.  
592 <https://doi.org/10.1111/gcb.13965>
- 593 Figueiredo, V., Enrich - Prast, A., & Rütting, T. (2016). Soil organic matter content controls  
594 gross nitrogen dynamics and N<sub>2</sub>O production in riparian and upland boreal soil. *European*  
595 *Journal of Soil Science*, *67*(6), 782–791. <https://doi.org/10.1111/ejss.12384>
- 596 Flörke, M., Schneider, C., & McDonald, R. I. (2018). Water competition between cities and  
597 agriculture driven by climate change and urban growth. *Nature Sustainability*, *1*, 51–58.  
598 <https://doi.org/10.1038/s41893-017-0006-8>
- 599 Food and Agricultural Organization of the United nations (FAO). FAOSTAT data. Retrieved  
600 June 18, 2018, from <http://www.fao.org/faostat/en/#data>
- 601 Gao, B., Huang, T., Ju, X., Gu, B., Huang, W., Xu, L., ... Cui, S. (2018). Chinese cropping  
602 systems are a net source of greenhouse gases despite soil carbon sequestration. *Global*  
603 *Change Biology*, *24*(12), 5590-5606. <https://doi.org/10.1111/gcb.14425>
- 604 Gao, S., Chang, D., Zou, C., Cao, W., Gao, J., Huang, J., ... Thorup-Kristensen, K. (2018).  
605 Archaea are the predominant and responsive ammonia oxidizing prokaryotes in a red  
606 paddy soil receiving green manures. *European Journal of Soil Biology*, *88*, 27–35.

- 607 <https://doi.org/https://doi.org/10.1016/j.ejsobi.2018.05.008>
- 608 Gerber, J. S., Carlson, K. M., Makowski, D., Mueller, N. D., Garcia de Corstazar-Atauri, I.,  
609 Havlík, P., ... West, P. C. (2016). Spatially explicit estimates of N<sub>2</sub>O emissions from  
610 croplands suggest climate mitigation opportunities from improved fertilizer management.  
611 *Global Change Biology*, 22(10), 3383–3394. <https://doi.org/10.1111/gcb.13341>
- 612 Guan, D., Meng, J., Reiner, D. M., Zhang, N., Shan, Y., Mi, Z., ... Davis, S. J. (2018).  
613 Structural decline in China's CO<sub>2</sub> emissions through transitions in industry and energy  
614 systems. *Nature Geoscience*, 11(8), 551–555. [https://doi.org/10.1038/s41561-018-0161-](https://doi.org/10.1038/s41561-018-0161-1)  
615 1
- 616 International Fertilizer Association (IFA). IFA database. Retrieved June 18, 2018, from  
617 <http://ifadata.fertilizer.org/ucSearch.aspx>
- 618 IPCC. (2006). *Guidelines for National Greenhouse Gas Inventories*.  
619 [https://doi.org/http://www.ipcc-](https://doi.org/http://www.ipcc-nggip.iges.or.jp/public/2006gl/pdf/2_Volume2/V2_3_Ch3_Mobile_Combustion.pdf)  
620 [nggip.iges.or.jp/public/2006gl/pdf/2\\_Volume2/V2\\_3\\_Ch3\\_Mobile\\_Combustion.pdf](https://doi.org/http://www.ipcc-nggip.iges.or.jp/public/2006gl/pdf/2_Volume2/V2_3_Ch3_Mobile_Combustion.pdf)
- 621 Ito, A., & Inatomi, M. (2012). Use of a process-based model for assessing the methane budgets  
622 of global terrestrial ecosystems and evaluation of uncertainty. *Biogeosciences*, 9(2), 759–  
623 773. <https://doi.org/10.5194/bg-9-759-2012>
- 624 Jäger, N., Stange, C. F., Ludwig, B., & Flessa, H. (2011). Emission rates of N<sub>2</sub>O and CO<sub>2</sub> from  
625 soils with different organic matter content from three long-term fertilization  
626 experiments—a laboratory study. *Biology and Fertility of Soils*, 47(5), 483.  
627 <https://doi.org/10.1007/s00374-011-0553-5>
- 628 Janssens-Maenhout, G., Crippa, M., Guizzardi, D., Muntean, M., Schaaf, E., Dentener, F., ...  
629 Petrescu, A. M. R. (2017). EDGAR v4.3.2 Global Atlas of the three major Greenhouse  
630 Gas Emissions for the period 1970–2012. *Earth System Science Data Discussions*.  
631 <https://doi.org/10.5194/essd-2017-79>

- 632 Jiang, C., Lu, D., Zu, C., Shen, J., Wang, S., Guo, Z., ... Wang, H. (2018). One-time root-zone  
633 N fertilization increases maize yield, NUE and reduces soil N losses in lime concretion  
634 black soil. *Scientific Reports*, 8(1), 10258. <https://doi.org/10.1038/s41598-018-28642-0>
- 635 Li, C., Zhuang, Y., Cao, M., Crill, P., Dai, Z., Frohking, S., ... & Wang, X. (2001). Comparing  
636 a process-based agro-ecosystem model to the IPCC methodology for developing a  
637 national inventory of N<sub>2</sub>O emissions from arable lands in China. *Nutrient Cycling in*  
638 *Agroecosystems*, 60(1-3), 159-175. <https://doi.org/10.1023/A:101264220>
- 639 Liu, J., Kuang, W., Zhang, Z., Xu, X., Qin, Y., Ning, J., ... Chi, W. (2014). Spatiotemporal  
640 characteristics, patterns and causes of land use changes in China since the late 1980s. *Acta*  
641 *Geographica Sinica*, 69(1), 3–14. <https://doi.org/10.11821/dlxb201401001>
- 642 Lu, C., & Tian, H. (2017). Global nitrogen and phosphorus fertilizer use for agriculture  
643 production in the past half century: Shifted hot spots and nutrient imbalance. *Earth System*  
644 *Science Data*, 9(1), 181–192. <https://doi.org/10.5194/essd-9-181-2017>
- 645 Ma, L., Shan, J., & Yan, X. (2015). Nitrite behavior accounts for the nitrous oxide peaks  
646 following fertilization in a fluvo-aquic soil. *Biology and Fertility of Soils*, 51(5), 563–572.  
647 <https://doi.org/10.1007/s00374-015-1001-8>
- 648 Ministry of Agriculture of the People's Republic of China. *Regional Planning of Advantageous*  
649 *Agricultural Products (2003-2007)*. Retrieved March 18, 2018, from  
650 [http://www.moa.gov.cn/ztlz/ysncpqybjgh/200302/t20030212\\_54322.htm](http://www.moa.gov.cn/ztlz/ysncpqybjgh/200302/t20030212_54322.htm)
- 651 Myhre, G., Shindell, D., Breon, F.-M., Collins, W., Fuglestedt, J., Huang, J., ... Zhang, H.  
652 (2013). Anthropogenic and Natural Radiative Forcing. In: Stocker, T. F., Qin, G.-K.  
653 Plattner, M. Tignor, S. K. Allen, J. Boschung, A. Nauels, Y. Xia, V. Bex & P. M. Midgley  
654 (eds.), *Climate Change 2013: The Physical Science Basis. Contribution of Working Group*  
655 *I to the Fifth Assessment Report of the Intergovernmental Panel on Climate Change*.  
656 Cambridge University Press, Cambridge, United Kingdom and New York, NY, USA,



- 657 1535 pp, doi:10.1017/CBO9781107415324.
- 658 National Development and Reform Commission (NDRC). *China's National Climate Change*  
659 *Program*. Retrieved March 18, 2018, from [http://www.china-](http://www.china-un.org/eng/gyzg/t626117.htm)  
660 [un.org/eng/gyzg/t626117.htm](http://www.china-un.org/eng/gyzg/t626117.htm)
- 661 Paustian, K., Lehmann, J., Ogle, S., Reay, D., Robertson, G. P., & Smith, P. (2016). Climate-  
662 smart soils. *Nature*, 532(7597), 49–57. <https://doi.org/10.1038/nature17174>
- 663 Perlman, J., Hijmans, R. J., & Horwath, W. R. (2014). A metamodelling approach to estimate  
664 global N<sub>2</sub>O emissions from agricultural soils. *Global Ecology and Biogeography*, 23(8),  
665 912–924. <https://doi.org/10.1111/geb.12166>
- 666 Pettitt, A. N. (1979). A Non-Parametric Approach to the Change-Point Problem. *Applied*  
667 *Statistics*, 28(2), 126–135. <https://doi.org/10.2307/2346729>
- 668 Philibert, A., Loyce, C., & Makowski, D. (2012). Quantifying Uncertainties in N<sub>2</sub>O Emission  
669 Due to N Fertilizer Application in Cultivated Areas. *PLoS ONE*, 7(11), e50950.  
670 <https://doi.org/10.1371/journal.pone.0050950>
- 671 Ravishankara, A. R., Daniel, J. S., & Portmann, R. W. (2009). Nitrous oxide (N<sub>2</sub>O): The  
672 dominant ozone-depleting substance emitted in the 21st century. *Science*, 326(5949),  
673 123–125. <https://doi.org/10.1126/science.1176985>
- 674 Richards, M., Butterbach-Bahl, K., Jat, M. L., Ortiz-Monasterio, I., Sapkota, T., & Lipinski,  
675 B. (2015). *Site-Specific Nutrient Management: Implementation guidance for*  
676 *policymakers and investors*. <https://doi.org/10.1177/002204269702700108>
- 677 Saikawa, E., Prinn, R. G., Dlugokencky, E., Ishijima, K., Dutton, G. S., Hall, B. D., ... Elkins,  
678 J. W. (2014). Global and regional emissions estimates for N<sub>2</sub>O. *Atmospheric Chemistry*  
679 *and Physics*, 14(9), 4617–4641. <https://doi.org/10.5194/acp-14-4617-2014>
- 680 Sandor, R., Ehrhardt, F., Brilli, L., Carozzi, M., Recous, S., Smith, P., ... Bellocchi, G. (2018).  
681 The use of biogeochemical models to evaluate mitigation of greenhouse gas emissions

- 682 from managed grasslands. *Science of the Total Environment*, 642, 292-306.  
683 <https://doi.org/10.1016/j.scitotenv.2018.06.020>
- 684 Shcherbak, I., Millar, N., & Robertson, G. P. (2014). Global metaanalysis of the nonlinear  
685 response of soil nitrous oxide (N<sub>2</sub>O) emissions to fertilizer nitrogen. *Proceedings of the*  
686 *National Academy of Sciences*, 111(25), 9199–9204.  
687 <https://doi.org/10.1073/pnas.1322434111>
- 688 Song, X., Liu, M., Ju, X., Gao, B., Su, F., Chen, X. & Rees, R. M. (2018). Nitrous oxide  
689 emissions increase exponentially when optimum nitrogen fertilizer rates are exceeded in  
690 the North China Plain. *Environmental Science & Technology*, 52(21), 12504-12513.  
691 <https://doi.org/10.1021/acs.est.8b03931>
- 692 Sun, W., & Huang, Y. (2012). Synthetic fertilizer management for China's cereal crops has  
693 reduced N<sub>2</sub>O emissions since the early 2000s. *Environmental Pollution*, 160, 24–27.  
694 <https://doi.org/10.1016/j.envpol.2011.09.006>
- 695 The National Development and Reform Commission. *The People's Republic of China National*  
696 *Greenhouse Gas Inventory in 2005*. China Environmental Science Press.
- 697 Tian, H., Chen, G., Lu, C., Xu, X., Hayes, D. J., Ren, W., ... Wofsy, S. C. (2015). North  
698 American terrestrial CO<sub>2</sub> uptake largely offset by CH<sub>4</sub> and N<sub>2</sub>O emissions: toward a full  
699 accounting of the greenhouse gas budget. *Climatic Change*, 129(3–4), 413–426.  
700 <https://doi.org/10.1007/s10584-014-1072-9>
- 701 Tian, H., Lu, C., Ciais, P., Michalak, A. M., Canadell, J. G., Saikawa, E., ... Wofsy, S. C.  
702 (2016). The terrestrial biosphere as a net source of greenhouse gases to the atmosphere.  
703 *Nature*, 531(7593), 225–228. <https://doi.org/10.1038/nature16946>
- 704 Tian, H., Yang, J., Lu, C., Xu, R., Canadell, J. G., Jackson, R. B., ... Zhu, Q. (2018). The  
705 Global N<sub>2</sub>O Model Intercomparison Project. *Bulletin of the American Meteorological*  
706 *Society*, 99(6), 1231–1251. <https://doi.org/10.1175/BAMS-D-17-0212.1>

- 707 Tian, H., Yang, J., Xu, R., Lu, C., Canadell, J. G., Davidson, E. A., ... & Gerber, S. (2019).  
708 Global soil nitrous oxide emissions since the preindustrial era estimated by an ensemble  
709 of terrestrial biosphere models: Magnitude, attribution, and uncertainty. *Global Change*  
710 *Biology*, 25(2), 640-659. <https://doi.org/10.1111/gcb.14514>
- 711 USEPA (2012). *Global Anthropogenic Non-CO<sub>2</sub> Greenhouse Gas Emissions: 1990 - 2030*.  
712 *Office of Atmospheric Programs Climate Change Division U.S. Environmental Protection*  
713 *Agency*. [https://doi.org/EPA 430-R-12-006](https://doi.org/EPA%20430-R-12-006)
- 714 Van Drecht, G., Bouwman, A. F., Knoop, J. M., Beusen, A. H. W., & Meinardi, C. R. (2003).  
715 Global modeling of the fate of nitrogen from point and nonpoint sources in soils,  
716 groundwater, and surface water. *Global Biogeochemical Cycles*, 17(4), 1115.  
717 <https://doi.org/10.1029/2003GB002060>
- 718 Vet, R., Artz, R. S., Carou, S., Shaw, M., Ro, C. U., Aas, W., ... Reid, N. W. (2014). A global  
719 assessment of precipitation chemistry and deposition of sulfur, nitrogen, sea salt, base  
720 cations, organic acids, acidity and pH, and phosphorus. *Atmospheric Environment*, 93, 3–  
721 100. <https://doi.org/10.1016/j.atmosenv.2013.10.060>
- 722 Wang, R., Goll, D., Balkanski, Y., Hauglustaine, D., Boucher, O., Ciais, P., ... Tao, S. (2017).  
723 Global forest carbon uptake due to nitrogen and phosphorus deposition from 1850 to 2100.  
724 *Global Change Biology*, 23(11), 4854–4872. <https://doi.org/10.1111/gcb.13766>
- 725 Wang, S., Luo, S., Li, X., Yue, S., Shen, Y., & Li, S. (2016). Effect of split application of  
726 nitrogen on nitrous oxide emissions from plastic mulching maize in the semiarid Loess  
727 Plateau. *Agriculture, Ecosystems and Environment*, 220, 21–27.  
728 <https://doi.org/10.1016/j.agee.2015.12.030>
- 729 Winiwarter, W., Höglund-Isaksson, L., Klimont, Z., Schöpp, W., & Amann, M. (2018).  
730 Technical opportunities to reduce global anthropogenic emissions of nitrous oxide.  
731 *Environmental Research Letters*, 13(1), 014011. <https://doi.org/10.1088/1748->

- 732 9326/aa9ec9
- 733 Xia, L., Lam, S. K., Wolf, B., Kiese, R., Chen, D., & Butterbach-Bahl, K. (2018). Trade-offs  
734 between soil carbon sequestration and reactive nitrogen losses under straw return in global  
735 agroecosystems. *Global Change Biology*, 24(12), 5919–5932.  
736 <https://doi.org/10.1111/gcb.14466>
- 737 Yue, Q., Cheng, K., Ogle, S., Hillier, J., Smith, P., Abdalla, M., ... & Pan, G. (2019). Evaluation  
738 of four modelling approaches to estimate nitrous oxide emissions in China's cropland.  
739 *Science of the Total Environment*, 652, 1279–1289.  
740 <https://doi.org/10.1016/j.scitotenv.2018.10.336>
- 741 Yue, Q., Ledo, A., Cheng, K., Albanito, F., Lebender, U., Sapkota, T. B., ... & Pan, G. (2018).  
742 Re-assessing nitrous oxide emissions from croplands across Mainland China. *Agriculture,  
743 Ecosystems and Environment*, 268, 70–78. <https://doi.org/10.1016/j.agee.2018.09.003>
- 744 Zaehle, S., & Friend, A. D. (2010). Carbon and nitrogen cycle dynamics in the O-CN land  
745 surface model: 1. Model description, site-scale evaluation, and sensitivity to parameter  
746 estimates. *Global Biogeochemical Cycles*, 24(1), GB1005.  
747 <https://doi.org/10.1029/2009GB003521>
- 748 Zhang, B., Tian, H., Lu, C., Dangal, S. R. S., Yang, J., & Pan, S. (2017). Global manure  
749 nitrogen production and application in cropland during 1860–2014: A 5 arcmin gridded  
750 global dataset for Earth system modeling. *Earth System Science Data*, 9(2), 667–678.  
751 <https://doi.org/10.5194/essd-9-667-2017>
- 752 Zhang, Y. L., Fan, J. B., Wang, D. S., & Shen, Q. R. (2009). Genotypic Differences in Grain  
753 Yield and Physiological Nitrogen Use Efficiency Among Rice Cultivars. *Pedosphere*,  
754 19(6), 681–691. [https://doi.org/10.1016/S1002-0160\(09\)60163-6](https://doi.org/10.1016/S1002-0160(09)60163-6)
- 755 Zhou, F., Shang, Z., Ciais, P., Tao, S., Piao, S., Raymond, P., ... & Peng, S. (2014). A new  
756 high-resolution N<sub>2</sub>O emission inventory for China in 2008. *Environmental science &*

- 757            *technology*, 48(15), 8538-8547. <https://doi.org/10.1021/es5018027>
- 758    Zhou, F., Shang, Z., Zeng, Z., Piao, S., Ciais, P., Raymond, P. A., ... Mao, Q. (2015). New  
759            model for capturing the variations of fertilizer-induced emission factors of N<sub>2</sub>O. *Global*  
760            *Biogeochemical Cycles*, 29(6), 885–897. <https://doi.org/10.1002/2014GB005046>
- 761    Zhu, X., Li, Y., Li, M., Pan, Y., & Shi, P. (2013). Agricultural irrigation in China. *Journal of*  
762            *Soil and Water Conservation*, 68(6), 147–154. <https://doi.org/10.2489/jswc.68.6.147A>
- 763    Zou, J., Lu, Y., & Huang, Y. (2010). Estimates of synthetic fertilizer N-induced direct nitrous  
764            oxide emission from Chinese croplands during 1980–2000. *Environmental Pollution*,  
765            158(2), 631-635. <https://doi.org/10.1016/j.envpol.2009.08.026>
- 766    Zuo, L., Zhang, Z., Carlson, K. M., MacDonald, G. K., Brauman, K. A., Liu, Y., ... & Wang,  
767            X. (2018). Progress towards sustainable intensification in China challenged by land-use  
768            change. *Nature Sustainability*, 1(6), 304-313. <https://doi.org/10.1038/s41893-018-0076-2>